

A Comparison of Different Test Techniques on Fatigue Threshold Behavior of Surface Flaws in a Titanium Alloy

S. MALL*, D. A. NAGY** and J. R. JIRA***

*Department of Aeronautics and Astronautics, Air Force Institute of Technology, Wright-Patterson AFB, OH 45433, USA

**Department of Engineering Mechanics, USAF Academy, Colorado Springs, CO 80332, USA

***AFWAL Materials Laboratory, Wright-Patterson AFB, OH 45433, USA

ABSTRACT

Two test types were conducted to examine the effects of different loading histories, closure loads and stress ratios on fatigue threshold of a titanium alloy. Both test types maintained a constant maximum stress intensity factor, K_{max} , but one with increasing minimum stress intensity factor, K_{min} , and other with decreasing K_{min} . The results of these tests were compared to the results of a previous study using the ASTM standard threshold measurement test (constant R and decreasing ΔK) and another threshold test with constant R and increasing ΔK . Analysis of the data indicated that threshold stress intensity factors (ΔK_{th}) were dependent on stress ratio. The effective threshold stress intensity factors adjusted for closure, ΔK_{effth} , were not dependent on stress ratio.

KEYWORDS

Fatigue threshold; fatigue crack propagation; closure; surface flaw; titanium alloy

INTRODUCTION

The structural components in many applications are subjected to high cycle fatigue crack growth, particularly in the near-threshold region (10^{-10} m/cycle). It is, therefore, important to determine the near-threshold crack behavior for these high cycle fatigue limited components for accurate life predictions. In addition to this, determining the threshold stress intensity factor below which a crack will not grow (ΔK_{th}), is important in predicting component life.

The ASTM recommended method (1986) for determining ΔK_{th} is a load shedding test. During the load shedding test a specimen with a propagating crack is subjected to a decreasing stress intensity, ΔK , at a constant stress ratio, R ($\sigma_{min}/\sigma_{max}$). This results in a decreasing crack growth rate.

The ΔK_{th} is then determined when the crack growth rate reaches the threshold level of 10^{-10} m/cycle. Tests attempting to measure a standard ΔK_{th} to be used for material life predictions have found threshold stress intensity values depending on reduction rate of ΔK , test frequency, environment, and stress ratio (Cadman et al., 1981; Doker et al., 1981; Doker and Peters, 1984; Herman et al., 1987). These studies, thus, showed that the measured ΔK_{th} values are dependent on loading history, crack closure, and plastic zone size.

In a recent study, Jira et al. (1988a) found that crack growth rates obtained at different stress ratios tend to merge to a single curve using a stress intensity adjusted for crack closure, $\Delta K_{eff} = K_{max} - K_{cl}$. These researchers also found that effective threshold stress intensity values, ΔK_{effth} , were approximately equal for different stress ratios. This study showed the possibility of using ΔK_{effth} as a material property in the near-threshold crack growth region. There is obviously a need to determine if similar results are obtained under different loading histories, and crack closure effects. In addition, there is a need to determine if results obtained from threshold test with initially propagating cracks are applicable to materials with initially non-propagating cracks.

The objective of the present study was, therefore, to investigate the effects of two loading histories on near-threshold fatigue crack growth behavior (both threshold stress intensity and crack closure) of surface flaws in a titanium alloy. Two type of load histories were examined. The first type maintained a constant maximum stress intensity factor, K_{max} , on a specimen with a growing crack. As the crack grew, the minimum stress intensity factor, K_{min} , was increased until the crack growth rate reached the threshold level. The second type also maintained a constant K_{max} with a non-growing crack. Here the K_{min} was decreased until the crack started to grow. This paper provides the details and results of these tests.

TESTING PROCEDURE

Specimen Preparation

A high strength titanium alloy, Ti-6Al-2Sn-4Zr-6Mo was tested. The details of chemical composition and heat-treatment are the same as was used in a previous study (Jira, et al., 1988a). The testing was performed using specimen geometry having rectangular cross-section with a surface flaw. The gage sections of the specimens were electropolished to a minimum depth of 0.2 mm to eliminate surface residual stresses and roughness produced during machining. A semicircular electro-discharge (EDM) notch, approximately 250 μ m wide and 80 μ m high and 125 μ m deep, was machined on each specimen for crack initiation. All specimens were precracked to ensure there was no residual stress effects from the EDM notching. The crack was initiated and grown a distance equal to the radius of the notch (0.1 mm) to ensure a proper starter crack. The precracking was accomplished using a constant maximum load and constant stress ratio, R. All specimens were precracked with R = -1.0 to maintain a constant loading history. The maximum stress for precracking varied between 0.2 σ_{ys} and 0.3 σ_{ys} (σ_{ys} = 1158 MPa). The selected precracking maximum load was chosen so it would not exceed the initial maximum load of the tests and induce an overload condition.

Test Set-Up

All tests were run on an MTS machine at room temperature (23°C) under a fully automated computer controlled mode. A laser interferometer displacement gage (IDG) was used to get accurate measurements of crack lengths ($\approx 2\mu$ m) and near crack tip surface closure loads (Hartman and Nicholas, 1987). The IDG system produced load-crack mouth opening displacement (CMOD) curves at selected intervals during the test which were used to determine both crack length and closure loads. Crack length was calculated from the elastic compliance determined from the slope of a straight line fitted to the linear portion of the curve. The compliance for this specimen with the same type of crack length was established by Matheck et al., (1983). The crack closure load was determined as the load at which the load-CMOD curve displayed the first deviation from linearity on unloading. To backup the IDG crack length measurements, optical measurements of the cracks were made continuously during the test using a traveling microscope.

Test Plan

Two test techniques were employed to examine the influences of prior loading history on threshold as elaborated in the following.

Constant K_{max} and Increasing K_{min} Test

This test involved the application of a constant K_{max} with a increasing K_{min} to a propagating crack. The K_{min} was increased linearly with crack length, through fully automated computer control, until threshold crack growth rate (1×10^{-10} m/cycle) was obtained (Fig. 1). Once threshold crack growth was reached, the test was continued at threshold R under constant maximum load to measure, near-threshold growth rate.

This test was run twice at different stress ratios on separate specimens to measure the effects of loading history and different closure loads. During the first test K_{max} was 5.0 MPa/m with an initial R of 0.1. The specimen reached threshold crack growth rate at R = 0.59. During the second test K_{max} was 4.0 MPa/m and the initial R was -0.3. Threshold crack growth rate was reached at R = 0.44. Both tests were run at a frequency of 20 hertz.

Constant K_{max} Decreasing K_{min} Test

This test involved constant K_{max} and initial K_{min} (Fig. 1) which ensured that there was no apparent crack growth or the crack was growing well below the threshold rate. During this test, initiation of crack growth was defined arbitrarily when the growth rate reached a value of 5×10^{-11} m/cycle. The K_{min} was applied over a block of 198,500 cycles while the IDG checked for crack propagation. Thirty crack length measurements were made using the IDG system which provided the crack growth rate. If the crack growth rate was below the 5×10^{-11} m/cycle, the stress ratio was decreased and another block of cycles was applied (Fig. 2). This process was continued until the assumed threshold crack growth rate level of 5×10^{-11} m/cycle was reached. The 198,000 cycles in each block were selected to allow the crack to grow a sufficient amount that the IDG would be able to measure any crack growth that may occur within its 2 μ m resolution capability. Once crack growth rate was detected more than 5×10^{-11} m/cycle,

the crack was grown under constant maximum load at the existing R to measure near-threshold crack growth.

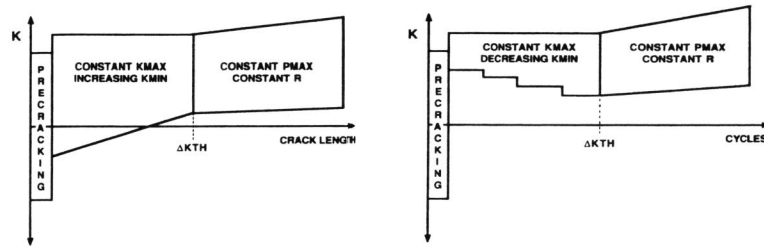


Fig. 1. Schematic of loading history used in two test types in experimental investigation.

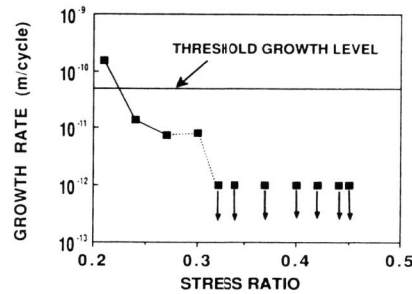


Fig. 2. Crack growth rates as function of R

This test was run twice at different stress ratios to examine the effects of loading history and different closure loads. The first test was run with K_{max} of 6.0 MPa/m and initial R of 0.70. The R was decreased in increments of 0.02 for each block of cycles. The crack growth rate increased above the 5×10^{-11} m/cycle at R = .59. The second decreasing K_{min} test was run at $K_{max} = 4.0$ MPa/m and R was initially 0.44. The R was decreased until the crack growth above 5×10^{-11} m/cycle occurred at R = 0.21 as shown in Fig. 2. Both of these tests were run at a frequency of 20 hertz.

RESULTS AND DISCUSSIONS

Typical crack growth data from a constant K_{max} and increasing K_{min} tests are shown in Fig. 3. This test employed initially $R = -0.3$ and reached threshold at R = 0.44. After determining threshold, test was continued at

the constant load, P_{max} and $R = 0.44$ obtained at threshold. Figure 4 shows the same crack growth rate curves adjusted for closure. The lines in these figures represents the average trend for data obtained from CT specimens from a previous study (Jira et al., 1988a) on the same material for $R = 0.1$ and $R = 0.5$. It can be seen from Fig. 4 that growth data for both the constant K_{max} and increasing K_{min} test and constant P_{max} constant R test shifted to left and consolidated into a single curve. This is similar to CT data with constant R tests. Further, surface flaw and CT data for $R = 0.5$ are in reasonable agreement with each other once closure effect is accounted for below the growth rate of 10^{-9} m/cycle as shown in Fig. 4. The initial data which do not fall into a single curve in Fig. 4 from increasing K_{min} test represents negative values of R. This lack of consolidation of the data into a single curve may be due to inability to determine the true closure load from load-CMOD data on a surface geometry. The measured value of effective threshold stress intensity, ΔK_{eff} from this test was 2.54. This value agrees with its counterpart from CT specimens. The other test involving K_{max} and increasing K_{min} had initial $R = 0.1$ and threshold $R = 0.59$. This second test provided essentially the same behavior as the first one as elaborated above except for the fact that no crack closure was measured by the IDG system between the stress ratios of 0.2 and 0.4. However, since the stress ratio was large near threshold, closure was not expected to be observed at threshold in this test. Further, the effective threshold stress, ΔK_{eff} from this second test involving increasing K_{min} was 2.44 which agrees with previous test and from CT specimens.

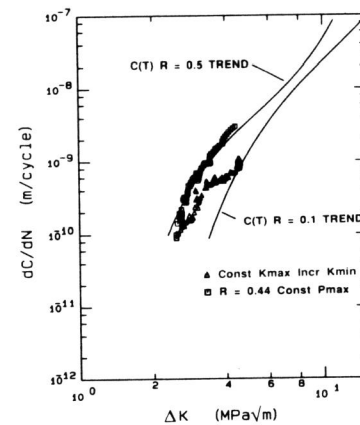


Fig. 3. Crack growth rate versus ΔK for increasing K_{min} test.

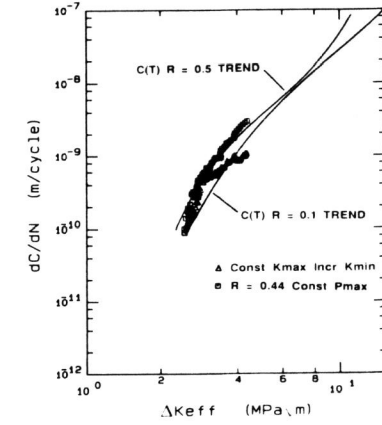


Fig. 4. Crack growth rate versus ΔK_{eff} for increasing K_{min} test.

Figure 5 shows the crack growth data obtained from the constant K_{max} test with initial $R = 0.44$. The stress ratio was decreased in each block of 198000 cycles till growth of 5×10^{-11} m/cycle was obtained which occurred at $R = 0.21$. The crack growth rates for each block of cycles are shown as

well as the crack growth curve for the constant maximum load and stress ratio (0.21) portion of this test. In this test since the stress ratios were large initially, closure was not expected to develop, but as the stress ratios decreased to $R = 0.21$ closure should have developed. However, the IDG system did not again measure any closure for $0.2 < R < 0.4$. This resulted in the effective value of 3.18 well above all other measured value in this study and from CT specimen (Jira et al., 1988). In fact, if the crack closure was present (and had been measured), both the effective threshold value and the growth rate data would have been consistent with the remaining data using an effective stress intensity factor. This would lead one to believe that closure may not be easily detected in surface flaws for $0.20 < R < 0.4$. For larger values of R , there is no apparent closure for this material. For smaller values of R , closure is readily detected. In this intermediate region, the extent of closure may be inadequate to detect with a mouth opening displacement gage, no matter how precise it is. On the other hand, in the second test involving constant K_{max} and decreasing K_{min} test with initial $R = 0.7$, the threshold was obtained at 0.59. This test resulted in ΔK_{eff} of 2.38 which is in agreement with other measured values in this study and with CT specimens.

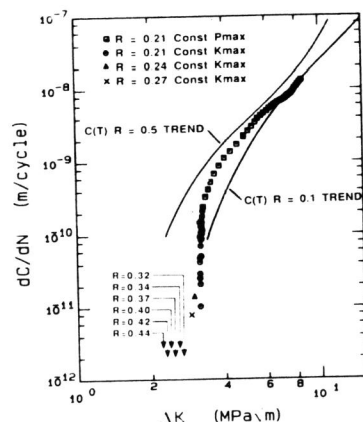


Fig. 5. Crack growth rate versus ΔK for decreasing K_{min} test

The two test technique employed in this study were selected to evaluate the role of prior loading history on the threshold under both decreasing and increasing ΔK test conditions. In both type of tests, the plastic zone ahead of the crack was kept constant but larger than the one obtained during precracking as threshold is approached with decreasing and increasing ΔK loading. In the ASTM recommended test, the crack is grown into a region with a plastic zone size which is larger than created by new crack growth. Guidelines have been developed to minimize or eliminate completely the loading history effect by controlling the rate of load shedding. Fatigue crack growth threshold tests have been conducted by using the ASTM recommended load shedding technique using the similar surface flaw specimen geometry of the same titanium alloy employed in the present study

(Jira et al., 1988b). The ASTM method involves decreasing ΔK with constant R . Further, this previous study (Jira et al., 1988b) also included increasing ΔK tests with constant R . The results of this previous and present study show that there appears to be a single value of effective threshold stress intensity factor, ΔK_{eff} which is independent of stress ratio, R or load history. This average value of ΔK_{eff} is about 2.30 MPa/m. Further, ΔK_{eff} obtained from surface flaw and CT specimens are in agreement with each other. Therefore, the results of present and previous studies (Jira et al., 1988b) clearly show that loading history can be completely accounted for in the threshold regime if crack closure is taken into account.

CONCLUDING REMARKS

To examine the effects of different loading histories, closure loads, and stress ratios, two types of constant K_{max} tests were conducted. The first constant K_{max} test increased K_{min} and hence R , with crack growth until the threshold crack growth rate was reached. The second constant K_{max} test decreased K_{min} , and therefore R , with each block of applied cycles until the crack growth rate reached the threshold level. The effective threshold stress intensity factor which accounts for crack closure appears to be independent of stress ratio, loading history and test type. The crack growth rate curves adjusted for closure by using ΔK_{eff} obtained from different loading histories agreed with each other in the vicinity of threshold region i.e. less than 10^{-10} m/cycle. There was an apparent experimental difficulty in determining ΔK_{eff} for the tests which reached threshold at stress ratios between 0.2 and 0.4. This is believed to be due to the proximity of the closure load and the minimum load in these tests which resulted in a difficulty in resolving the true closure load. This appears to be an experimental limitation rather than a failure in the utility of the effective stress intensity.

ACKNOWLEDGMENT

The authors wish to thank Dr. T. Nicholas, USAF Metals Behavior Branch for the support and helpful suggestions.

REFERENCES

- ASTM Specification E647-86A (1986). Standard test methods for measurements of fatigue crack growth rates.
- Cadman, A.J., R. Brook and C.E. Nicholson (1981). Effect of test technique on the fatigue threshold ΔK_{th} . In: Fatigue thresholds: Fundamentals and Engineering Applications. (J. Backlund, A.F. Blom and C.J. Beevers, eds.), pp. 59-75. EMAS, U.K.
- Doker, H., V. Bachmann and G. Marci (1981). A comparison of different methods of determination of the threshold for fatigue crack propagation. In: Fatigue thresholds: Fundamentals and engineering applications. (J. Backlund, A.F. Blom and C.J. Beevers, eds.), pp. 275-285. EMAS, U.K.
- Doker, H. and M. Peters (1984). Fatigue threshold dependence on material environment and microstructure. In: Fatigue 84 (C.J. Beevers, ed.), pp. 275-285. EMAS, U.K.
- Hartman, G., and T. Nicholas (1987). An enhanced laser interferometer for precise displacement measurements. Experimental Techniques, 11, 24-26.

- Herman, W.A., R.W. Hertzberg and C.H. Newton (1987). A re-evaluation of fatigue threshold test methods. *Fatigue 87*, Vol II. (R.O. Ritchie and E.A. Starke Jr., eds.) pp. 819-828. EMAS, U.K.
- Jira, J.R., J. M. Larsen, and T. Nicholas (1988). Effects of closure on the fatigue crack growth of surface flaws in a titanium alloy. *Mechanics of Fatigue Crack Closure*, ASTM STP 982. (J.C. Newman and W. Elber, ed.) American society for testing and materials, Philadelphia.
- Jira, J.R., D.A. Nagy and T. Nicholas (1988). Influences of crack closure and load history on near-threshold crack growth behavior in surface flaws. Presented at ASTM symposium on Surface-crack growth: Models, Experiments and Structures, April 25, 1988, Sparks, Nevada.
- Mattheck, C., P. Morawietz, and D. Munz (1983). Stress intensity factor of the deepest point of a semi-elliptical surface crack in plates under stress gradients. *Int. J. Fracture* 23, 201-212.